

2023-10-02

# Electronic-photonic millimeter-wave sensing element based on monolithically integrated LNA and triple-cavity ring modulator

---

M. Singh, R. Wang, D. Onural, S. Buchbinder, H. Gevorgyan, V. Stojanovic, M. Popovic. 2023. "Electronic-photonic millimeter-wave sensing element based on monolithically integrated LNA and triple-cavity ring modulator" 49th European Conference on Optical Communications (ECOC 2023). <https://doi.org/10.1049/icp.2023.2586>

<https://hdl.handle.net/2144/48936>

*"Downloaded from OpenBU. Boston University's institutional repository."*

# Electronic-photonic millimeter-wave sensing element based on monolithically integrated LNA and triple-cavity ring modulator

Manuj Singh<sup>1</sup>, Ruocheng Wang<sup>2</sup>, Deniz Onural<sup>1</sup>, Sidney Buchbinder<sup>2</sup>, Hayk Gevorgyan<sup>1</sup>, Vladimir Stojanović<sup>2</sup> and Miloš A. Popović<sup>1</sup>

<sup>(1)</sup> Dept. of Electr. and Comp. Eng., Boston Univ., 8 St. Mary's St., Boston, MA, USA, [manujks@bu.edu](mailto:manujks@bu.edu)

<sup>(2)</sup> Dept. of Electrical Engineering and Computer Sciences, University of California, Berkeley, CA, USA

**Abstract** We demonstrate CMOS-integrated mm-wave-to-optical sensing elements comprising LNAs and triple-ring modulators that break the conversion-bandwidth tradeoff, showing a projected noise figure of 24 dB at 57 GHz (30 mW/element, -45 dBm RF-input, 6 dBm laser LO). The elements are tileable at small pitches, enabling photonic disaggregation of large-scale phased arrays. ©2023 The Author(s)

Large scale mm-wave antenna arrays have emerged as a key technology across several application domains that leverage high-bandwidth beamforming, ranging from 5G/6G+ communications to radar sensing. However, the performance scaling of these new systems depends heavily on the power-efficiency scaling of signal aggregation and processing across the arrays. Tight element pitch constraints are limiting both the per-element power dissipation and the available signal routing to the data processing subsystems. Limited per-element power dissipation leaves little room for local compute at the antenna element, or for ADCs and digital electrical links to carry the digitized data to downstream processing blocks.

These constraints significantly limit the array organization and architecture, and the types of algorithms that can be applied to the array data. Furthermore, the signal integrity of electrical links limits the size scaling of antenna arrays, and introduces unwanted electromagnetic radiation that interferes with radio signals of interest. These scaling issues are further exacerbated in future micro-cell and cell-free architectures, as well as air and space borne platforms where slow size, weight and power (SWaP) sensor arrays are needed. An efficient approach to direct antenna-to-photon transduction would enable disaggregation of compute and sensor elements. Integrated photonics based mm-wave links are a promising solution to overcome these scaling constraints<sup>[1]</sup>.

In this paper, we demonstrate a novel electronic-photonic integrated circuit (EPIC) based single-chip mm-wave sensing element composed of a low-noise amplifier (LNA) matched to and driving a high-speed triple-cavity electro-optic modulator at 57 GHz as shown in Fig. 3(a). A differential LNA is designed to

drive the outer cavities of the novel triple-ring modulator in a push-pull mode. The LNA consists of: cascaded active differential pairs with transformers to provide relatively high gain; an on-chip balun with impedance matching implemented at the input (to apply a single-ended RF signal); and an output matched to the impedance of the ring modulator. The compact mm-wave sensing element can be tiled at a pitch commensurate with array element spacings, and may enable a path to EPIC-enabled, revolutionary lightweight, large element count (1024+), low power, scalable disaggregated mm-wave phased array antennas for future communication and sensing systems – suitable to power and weight constrained ground, air and space platforms. The concept is in Fig. 1.

The mm-wave sensing element EPIC was fabricated in a commercial 45 nm SOI CMOS process (see micrograph in Fig. 2a). Traditional methods for electro-optic (EO) signal conversion rely on Mach-Zehnder modulators which are power hungry, and have large footprint incompatible with mm-wave array element pitches. Conventional microring-modulators offer smaller footprint and

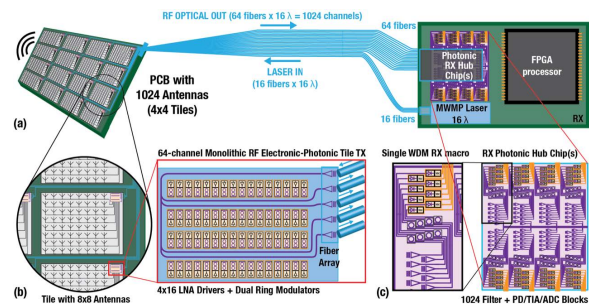


**Fig. 1: System concept:** (a) disaggregated mm-wave antenna panel connected to baseband processing hub via WDM photonic links based on monolithic EPICs and “photonic molecule” modulators; (b) 8×8 antenna tile feeding one photonic transmitter chip (16 λ × 4 ports = 64 channels), (c) photonic receiver hub chip with back-end processors. A multi wavelength, multi-port (MWMP) comb laser powers the links remotely.

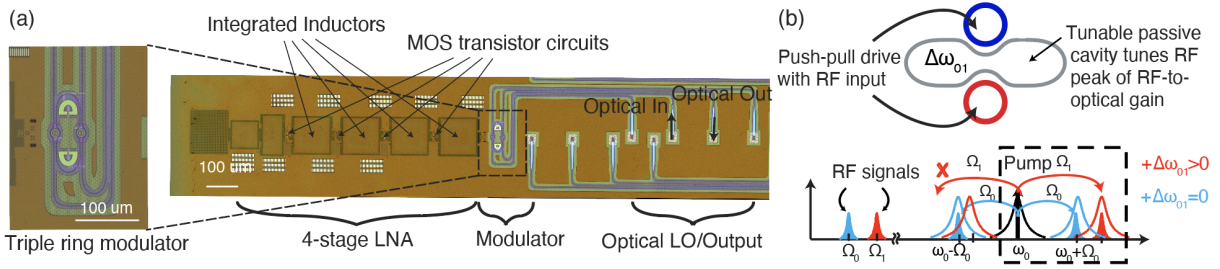


**Fig. 2: Monolithically integrated LNA+triple-cavity Si photonic modulator sensing element:** (a) Micrograph of sensing element, fabricated in GF 45RFSOI CMOS; (b) concept of off-resonant middle ring acting as tunable coupler, allows control of RF peak-gain frequency for efficient RF-optical conversion with any RF carrier frequency.

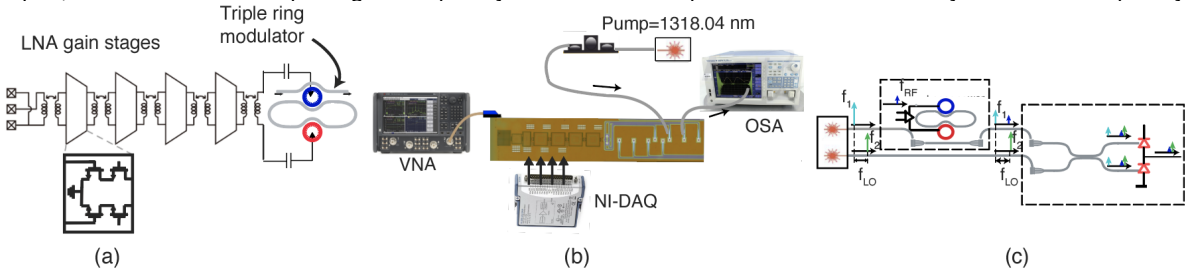


**Fig. 3:** (a) Schematic of the sensing element comprising an LNA driving a triple-ring modulator; (b) the experimental setup; (c) laser-forwarded coherent link with triple-ring modulators for improved noise figure.

lower power, but show a tradeoff between conversion efficiency (via high Q) and high RF carrier frequency (via low Q). Dual, coupled-cavity ring modulators based on the concept of a “photonic molecule” resonator resonance doublet<sup>[2]</sup> break this tradeoff and allow high carrier frequency with efficient conversion supported by small mode volume rings and resonance splitting. However, dual-cavity modulators are efficient at a single, fixed RF carrier frequency determined by the ring-ring coupling. This could be problematic if it is mismatched from the LNA’s peak gain frequency. Triple-ring modulators<sup>[3]</sup> (Fig. 2b) use a passive but tunable middle cavity to effect a variable coupling between outer active cavities, producing three supermodes/resonances at designed frequencies (blue spectrum in Fig. 2b, bottom). Controlling the supermode spacing allows for peak gain at a tunable RF carrier frequency while preserving the high conversion efficiency.

The resonance of the middle ring affects supermode frequencies. When we detune the middle ring by  $\Delta\omega_{01}$ , the central supermode is fixed but the outer supermode resonances shift to higher frequencies (red in Fig. 2b). This allows only one pair of supermode (SM) resonance frequencies to match to the desired RF frequency (e.g.  $\Omega_1$ ), suppressing the other sideband while preserving substantial field overlap of the two SM resonances. This results in the tunable single-sideband generation (dashed black box).

A vertical pn junction<sup>[4]</sup> is integrated into outer active cavities of the triple-ring modulator for

high shift efficiency while also enabling differential drive in push-pull mode. We tune the middle ring of the triple-cavity modulator to adjust the SM splitting and finally match the peak gain frequency of the LNA at 57 GHz to maximize the RF-to-optical sideband conversion efficiency. This is its key advantage over the (fixed splitting) dual-cavity modulator design<sup>[2]</sup>.

Figure 3b shows the measurement setup with a fiber array connecting a CW laser to the chip, and the on-chip LNA amplifying the low RF power mm-wave signal incident from a network analyzer. Bias currents for the LNA and the ring heaters are set so that the SM splitting is matched with LNA gain frequency at 57 GHz. We envision, and use, a laser-forwarded coherent link to connect a mm-wave sensing element to a remote hub (Figure 3c). A comb laser source with tone spacing ( $f_{LO}$ ) sends a pump tone at optical frequency  $f_1$  to the photonic Tx, while sending the reference tone at frequency  $f_2$  to the photonic Rx. The LNA receives the mm-wave signal from the antenna and drives the modulator with the amplified signal. The modulator generates a sideband located  $f_{RF}$  away from the pump tone, which is close to the second laser tone (reference tone). On the processing site (photonic Rx), the sideband is combined with the reference laser tone through an optical coupler and down-converted to electrical photocurrent signal centered at  $f_{LO} - f_{RF}$  (a lower carrier frequency than  $f_{RF}$ ), through a balanced photodetector (PD), and then processed by the rest of the receiver front-end.

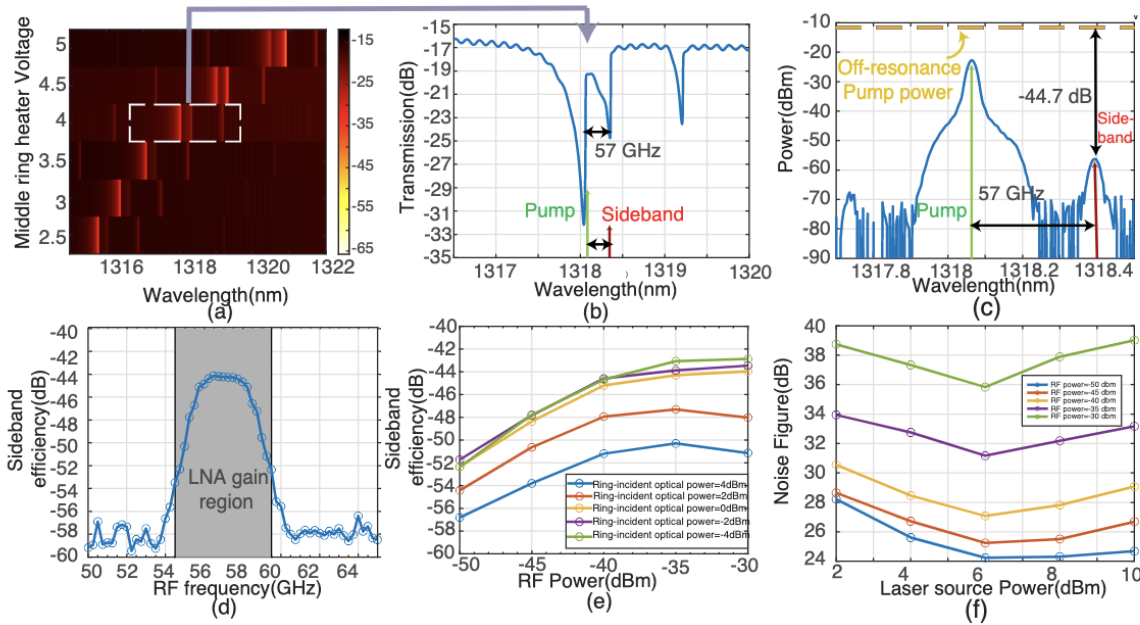


**Fig. 4:** (a) Modulator optical transmission spectrum mapped vs. middle ring detuning, achieving 57 GHz SM split for a pair of SM resonances; (b) spectrum for 57 GHz SM splitting case; (c) measured OSA spectrum showing -44.7 dB sideband efficiency at -40 dBm RF power and 5 dBm laser LO power. We define sideband efficiency as the ratio of sideband power to off-resonance in-waveguide pump power; (d) sideband efficiency vs. RF carrier frequency at -35 dBm RF power and 5 dBm laser power; (e) sideband efficiency vs. RF power for different ring-incident optical power; (f) projected noise figure for proposed link in Fig. 3 assuming 3 dB grating coupler loss.

Figure 4a shows the SM spacing tunability by means of thermo-optic tuning of the middle ring. We selected a particular operating condition, Fig. 4b, for the middle ring heater power to achieve SM splitting of 57 GHz to match the LNA's peak gain frequency. Figure 4c shows the sideband generation when the pump laser is tuned to 1318.06 nm with sideband efficiency of -44.7 dB at RF frequency of 57 GHz. The "sideband efficiency" in dB is the detected sideband power subtracted from the off-resonance pump power. Figure 4d shows the sideband efficiency versus RF frequency and highlights the gain region for the LNA from 54.5 GHz to 59.5 GHz with a peak at 57 GHz. In Fig. 4e, we observe the sideband efficiency measured at different RF and laser LO powers when the RF frequency is 57 GHz and the laser pump is fine-tuned around 1318.06 nm to attain the maximum sideband efficiency. At ring-incident optical powers above 0 dBm, there is notable self-heating induced compression and the sideband efficiency degrades. At an RF input power of -40 dBm the LNA enters a non-linear regime. Fig. 4f shows a projected Noise Figure (NF) of 24 dB projected using the measured data, operating at 57 GHz with -45 dBm RF power and 30 mW of LNA power. This is for the proposed laser-forwarded coherent link shown in Fig. 3c.

The NF degradation can be observed when the RF power level is above -35 dBm, as well as when the laser source power exceeds 6 dBm.

## Conclusions

We proposed a disaggregated large-scale phase array architecture enabled by compact, low-power mm-wave photonic sensing elements. The link architecture takes advantage of the compact size and supermode properties of triple-ring modulators, allowing WDM multiplexing of many antenna elements on a single fiber, enabling massive-scale signal remoting. The triple-ring resonator enables tuning to the LNA's peak RF gain while maintaining the high sideband efficiency advantage over single-ring modulators. Further optimization of doping implants and LNA-modulator co-design is expected to yield significant improvements of the NF by an additional 10-15 dB. We expect such mm-wave sensing elements to enable efficient transmission of mm-wave signals for large-scale array remoting in an integrated and compact package, enabling a photonic architecture for future large-scale MIMO arrays.

## Acknowledgements

Funded in part by the US Government. We thank Ayar Labs and GlobalFoundries for support related to 45RFSOI platform (AL11b test vehicle).

## References

- [1] P. Sanjari and F. Aflatouni, "An integrated photonic-assisted phased array transmitter for direct fiber to mm-wave links", *Nature Communications*, vol. 14, no. 1414, 2023. DOI: <https://doi.org/10.1038/s41467-023-37103-w>.
- [2] H. Gevorgyan, A. Khilo, and M. Popovic, "Efficient coupled-cavity electro-optic modulator on silicon for high carrier frequency, narrowband rf signals", in *Frontiers in Optics + Laser Science APS/DLS*, IEEE, 2019.
- [3] M. Singh, B. Zhang, D. Onural, H. Gevorgyan, and M. A. Popović, "Photonic molecule electro-optic modulators for efficient, widely tunable rf sideband generation and wavelength conversion", in *FIO 2021*, 2021. DOI: <https://doi.org/10.1364/FIO.2021.FTh6B.2>.
- [4] H. Gevorgyan, D. V. Orden, D. Onural, *et al.*, "High shift efficiency O-band spoked-ring modulator allowing fully electro-optic channel tuning in a 45nm CMOS platform", in *CLEO 2021*, 2021. DOI: [https://doi.org/10.1364/CLEO\\_SI.2021.SW3C.5](https://doi.org/10.1364/CLEO_SI.2021.SW3C.5).